Journal Pre-proof

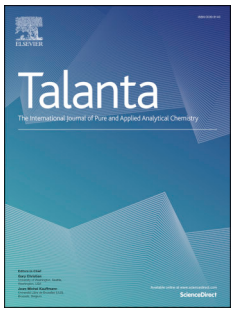

Accurate quantification of TiO_2 nanoparticles in commercial sunscreens using standard materials and orthogonal particle sizing methods for verification

Milica Velimirovic, Stephan Wagner, Fazel Abdolahpur Monikh, Toni Uusimäki, Ralf Kaegi, Thilo Hofmann, Frank von der Kammer

PII: S0039-9140(20)30212-5

DOI: https://doi.org/10.1016/j.talanta.2020.120921

Reference: TAL 120921

To appear in: *Talanta*

Received Date: 29 November 2019

Revised Date: 9 March 2020

Accepted Date: 10 March 2020

Please cite this article as: M. Velimirovic, S. Wagner, F.A. Monikh, T. Uusimäki, R. Kaegi, T. Hofmann, F.v.d. Kammer, Accurate quantification of TiO_2 nanoparticles in commercial sunscreens using standard materials and orthogonal particle sizing methods for verification, *Talanta* (2020), doi: https://doi.org/10.1016/j.talanta.2020.120921.

Accurate quantification of TiO_2 nanoparticles in commercial sunscreens using standard materials and orthogonal particle sizing methods for verification

Milica Velimirovic[1,2a], Stephan Wagner[1,3a], Fazel Abdolahpur Monikh[1], Toni Uusimäki[4], Ralf Kaegi[4], Thilo Hofmann[1*] and Frank von der Kammer[1*]

[1] *Department of Environmental Geosciences, Centre for Microbiology and Environmental Systems Science, University of Vienna, Althanstrasse 14, 1090 Vienna, Austria*
[2]*Ghent University, Department of Chemistry, Atomic & Mass Spectrometry – A&MS research group, Campus Sterre, Krijgslaan 281-S12, 9000 Ghent, Belgium*
[3]*UFZ - Helmholtz Centre for Environmental Research, Department of Analytical Chemistry, Permoserstrasse 15, 04318 Leipzig, Germany*
[4]*EAWAG, Swiss Federal Institute of Aquatic Science and Technology, Überlandstrasse 133, CH-8600 Dübendorf, Switzerland*

Corresponding authors: frank.kammer@univie.ac.at and thilo.hofmann@univie.ac.at

[a] both authors contributed equally to the manuscript

Revision submitted to Talanta

March 2020

Abstract

The implementation and enforcement of product labeling obligation as required, for example, by the cosmetic product regulation, needs simple and precise validated analytical methods. This also applies to the analysis of nanoparticles in products such as cosmetics. However, the provision of such methods is often hampered by inaccurate sizing due to unwanted nanoparticle changes, interference of matrix components with sizing and interactions between nanoparticles and analytical instrumentation. It is, therefore, necessary to develop appropriate sample preparation methods that preserve NP properties and reduce or remove matrix compounds that interfere with sizing. Further, accurate particle size analysis of samples containing unknown and possibly multiple nanoparticulate constituents is needed. In this study, we evaluated three sample preparation methods to identify and quantify TiO_2 nanoparticles in sunscreens. Specifically, we used a combination of ultracentrifugation and hexane washing, thermal destruction of the matrix, and surfactant assisted particle extraction. The method accuracy was assessed by two internal reference samples: pristine TiO_2 nanoparticles (NM104) and similar TiO_2 nanoparticles dispersed in a sunscreen matrix. The PSDs were determined using an asymmetrical flow field-flow fractionation hyphenated with multi-angle light scattering and inductively coupled plasma-mass spectroscopy. Particle sizing was based on size calibration of the particle retention time in the AF^4. Computation of radius of gyration from MALS data was used as an orthogonal particle sizing approach to verify ideal elution and particle size data from the AF^4 calibration. Among the three tested sample preparation methods surfactant assisted particle extraction revealed TiO_2 nanoparticle recoveries of above 90% and no increase in particle size due to sample preparation was observed. Finally, the sample preparation methods were applied to two commercial sunscreen samples revealing the existence of TiO_2-NP < 100 nm. Conclusively, the surfactant assisted particle extraction method can provide valid data for TiO_2-NPs in sunscreen and possibly for cosmetic samples of similar matrix.

Keywords: consumer products, cosmetics, product labeling, nanomaterial,

1 Introduction

Cosmetic products have to be labelled ”nano” according to the EU Cosmetic Product Regulation No. 1223/2009 when they contain nanomaterials [1]. This regulation defines nanomaterials or nanoparticles (NPs) as biopersistent and insoluble particles in a size range between 1 and 100 nm. To fulfill this regulation analytical methods have to be developed which allow assessing particle size and their quantity in cosmetics. This in turn requires dedicated sample preparation protocols and verified sizing methods [2–5]. However, quantitative, validated methods for the analysis of the particle size distribution (PSD) and the amount of NPs in cosmetic products are currently still absent.

Commercially available sunscreens represent a typical cosmetic emulsion matrix, representative for many different cosmetic products, which often contain TiO_2 particles in the nanosize range (UV filter) and other nano- to micro-size range particles like pigments. Laborious sample preparation methods for the analysis of TiO_2 particles in sunscreen have been extensively reported. They include different approaches being generally complex, time-consuming, altering the PSD and with a considerable environmental impact due to organic solvent extraction [6–8]. Recent advances are inverse supercritical fluid extraction [9]; and an ultrafiltration/ultracentrifugation method [10]. These methods are rather labor intensive and simple sample preparation procedures with marginal effects on particle size are still rare. In previous works TiO_2 particle sizing and quantification was done using a combination of field-flow fractionation (FFF) techniques hyphenated to either inductively coupled plasma–mass spectrometry (ICP-MS) for elemental analysis of Ti content or UV- and multi angle light scattering (MALS) detectors for size distribution [6–9,11]. Sample preparation may alter the PSD and the particle sizing method may not reproduce the actual PSD due to interferences between particles and the analytical method; thus, verification of both is necessary. Verification methods of particle sizing have been previously proposed e.g. by Cascio et al., (2015), Contado et al., (2013) and Wagner et al., (2015) [12,13,3]. Commonly they rely on external verification measurements e.g. analysis of well described reference materials or with electron microscopy analysis. However, an internal verification of size measurements would decrease analytical effort. For example, orthogonal verification of the particle sizing with asymmetrical flow field-flow fractionation (AF^4) could be accomplished by online MALS measurements. Additionally, well described reference materials are required to verify the sample preparation procedure, i.e. to

compare the known initial size distribution with the size distribution after sample preparation of the material. This allows the assessment of introduced changes in particle size by the sample preparation method.

In the present study, we evaluated three different approaches in sample preparation including (i) a combination of ultracentrifugation and hexane washing, (ii) thermal destruction of the matrix and (iii) the surfactant assisted particle extraction and dilution followed by particle stabilization. We identified the sample preparation method that is able to quantitatively assess TiO_2-NPs in sunscreens. For method evaluation we used a control sample with a comparable matrix and similar TiO_2-NPs compared to real sunscreen. The developed and tailored methods were then applied to real sunscreen samples. Particle size and concentration of TiO_2-NPs were determined with AF^4 hyphenated with MALS and ICP-MS. The PSD expressed as hydrodynamic size was derived from calibration of the AF^4 with particle size standards and verified by orthogonal particle sizing based on the analysis of the MALS signal. The accuracy of sample preparation method was confirmed by comparing the PSD of pristine TiO_2-NPs suspension and spiked sunscreen formulation with respect to mode, median and width (d_{10}, d_{90}).

2 Materials and methods

2.1 Materials, chemicals, standards

Hexane (99%), hydrogen peroxide (30% solution in water), nitric acid (HNO_3, 65%), boric acid, hydrofluoric acid (40%), hydrochloric acid (30%) and sodium hydroxide (NaOH) were of analytical grade (Merck, Germany). Ethanol absolute (99.98%) was purchased from VWR Chemicals, UK. Sodium dodecyl sulfate salt (99%) (SDS) was provided from Acros (New Jersey, USA). FL-70, a biodegradable detergent, was obtained from Fisher Scientific, US. Ultrapure water (MilliQ water) was produced by a Millipore Advantage A10 system equipped with a Bio-PakTM ultra-filter, 5000 g/mol molecular weight cut-off (Millipore, Billerica, USA). All carrier solutions used for AF^4 analyses were filtered before use (Anodisc < 0.02 µm filter, Whatman, Maidstone, UK).

2.2 Samples

In order to address the lack of missing reference material for TiO_2-NPs in cosmetic products, three types of samples were prepared and used to evaluate sample preparation methods (Table 1).

(1) A well-characterized TiO_2-material (NM104; JRC) consisting of TiO_2-NPs coated with Al_2O_3 and glycerol to adjust its hydrophilic properties was dispersed in a water/surfactant-mix and used as an internal reference sample during method development (referred to pristine TiO_2-NPs suspension in the following text). The dispersion protocol is provided in SI.1. (2) Particle-free sunscreen formulation contains no TiO_2 and other inorganic particles, but only the substances that make up a typical sunscreen emulsion. (3) Spiked sunscreen formulation consisting of (2) a known concentration of pristine TiO_2-NPs. The spiking procedure is provided in SI.1. The spiked sunscreen formulation was used to assess to what extent the sample preparation procedures alter the PSD of (1), the pristine TiO_2-NPs and what quantity of TiO_2-NPs can be extracted from the sunscreen matrix.

Two samples of sunscreens (Table 1) were used to test the developed sample preparation schemes. Ingredients in sunscreen A were TiO_2 particles in a water oil emulsion. In sunscreen B TiO_2 particles and iron oxide particles where dispersed in a water oil emulsion mimicking more complex cosmetic products with multiple particulate constituents.

2.3 Development of a sample preparation procedure for sunscreen containing TiO_2-NPs

A sample preparation method shall be selected which allows to determine the PSD with minimum alterations. It was not the scope to provide statistical data on reliability of the assessed methods; hence no replicate experiments were performed. The PSD including mode, median and width (d_{10}, d_{90}) of the pristine TiO_2 suspension was determined first. These data were used as a reference to detect changes in PSD due to the preparation methods of the spiked sunscreen. It is noted here, that validation of the best performing method will be the scope of a separate study.

2.3.1 Ultracentrifugation and hexane washing (method 1)

A mass of 5 g of each sunscreen sample (blank and spiked sunscreen formulation, sunscreen A and B) were diluted with 5 mL of MilliQ water and ultrasound sonicated in a water bath for 15 minutes. The sample mass was selected to simplify handling after ultracentrifugation. Aliquots (m = 3 g) of the diluted samples were decanted carefully in ultracentrifuge tubes and centrifuged using a Beckman Optima L-100 XP ultracentrifuge at 35,000 rpm (rotor SW 55 Ti; S/N 09E 2673, 55,000 rpm, force at r max: 368,000 g, k-factor 48) for 4 h. The supernatants were removed and 2 ml of n-hexane were added. The tubes were shaken by hand until the organic part formed a homogenous droplet. The droplets were removed and the residuals were transferred to a

15 mL centrifuge tube. The centrifuge tubes with the residuals were filled with 10 mL MilliQ water and 2 mL of 2wt% SDS solution. After vortex supported dispersion, it was centrifuged for 10 min at 4000 rpm. The supernatant was removed and all tubes were filled to 10 mL with 2wt% SDS solution. This dispersion was tip sonicated for 10 min. For further characterization with AF^4-MALS-ICP-MS the suspension was diluted 1:100 in MilliQ, pH was adjusted to 8-9 using 1 to 10 mM NaOH solution, and tip sonicated for 10 min (energy input 23,934 kJ in 15 ml volume).

2.3.2 Thermal combustion of the sunscreen (method 2)

A mass of 5 g of blank sunscreen formulation and spiked sunscreen formulation, sunscreen A and B were weighted in porcelain crucibles and placed in a muffle furnace. This amount of sunscreen ensured sufficient amount of ash for further treatment. The furnace temperature was slowly increased from room temperature to 550 °C in 1 h. The samples were combusted for 10 h under air. After combustion remaining matter was dispersed in 10 mL of 5%-SDS using tip-sonication. 1 mL of the dispersion was transferred into a 15 mL centrifuge vial and diluted with 3 mL of ethanol. The suspension was homogenized (Vortex + 10 min of water bath sonication) and subsequently centrifuged at 4,000 rpm for 10 min. The supernatant was removed, the remaining solids were dispersed in 2 mL of 10% SDS solutions and tip sonicated for 10 min. For further characterization with AF^4-MALS and AF^4-ICP-MS the suspension was diluted 1:100 in MilliQ water, pH was adjusted to 8-9 using 1 to 10 mM NaOH solution, and tip sonicated for 10 min (energy input 23,934 kJ in 15 ml volume).

2.3.3 Surfactant assisted particle extraction and dilution followed by particle stabilization (method 3)

Samples were prepared by a stepwise dilution of the sunscreen with a cleaning agent and particle stabilization step using the anionic surfactant. 10 mg of each sunscreen was weighted in a 10 mL glass vial and 1% (v/v) commercial household dish cleaning agent (Denk mit Ultra by DM) was added to give a sunscreen concentration of 1 mg/mL. The sample was shaken for 10 min horizontally until homogeneous appearance and subsequently sonicated for 15 min in an ultrasound water bath. 2 mL of the sonicated sample were transferred to an empty glass/plastic vial and 2 mL of 0.2wt% SDS solution were added (pH = 8.5-9). The sample was sonicated for 5

min and left overnight. After ultrasonication for 15 min in a water bath sonicator the sample was diluted 1:4 in 0.1 % (v/v) SDS and sonicated for 2 min.

2.3.4 Stability of the particle suspension

Dispersion stability of the extracted particles was evaluated by tracing the hydrodynamic diameter of the particles as a function of time within 60 minutes using dynamic light scattering (DLS) analysis. The particle size was considered as stable if the change in particle size did not exceed 10% within the test period. The stabilized suspension was further subjected to bulk analysis and NP characterization by AF^4-MALS, AF^4-ICP-MS and electron microscopy (EM).

2.4 Measurement and instrumentation

2.4.1 Total Ti and Fe analysis by ICP-OES

Total elemental content (Ti, Fe) of control samples and sunscreen samples have been determined after microwave assisted acid digestion. The samples were prepared for ICP-OES analysis using a high-pressure microwave system (Microwave 3000, Anton Paar, USA). Total digestion was performed in a two-step digestion by HNO_3, HCl, H_2O_2, and HF at a volumetric ratio of 5:2:1:1 (sample: $HCl:HNO_3:H_2O_2:HF$) followed by complexation of the remaining HF with H_3BO_3 (350 mg boric acid /15 mL of MilliQ water). Determinations of total Ti and Fe concentrations in the digested samples were carried out by ICP-OES (Optima 5300DV, PerkinElmer Inc., Waltham, USA) at a wavelength of 334.9 nm and 238.2 nm, respectively.

2.4.2 Dynamic light scattering and zeta potential measurements for pre-characterization

The DLS measurements were performed using a Malvern Zetasizer Nano ZS (Malvern instruments Ltd. with a laser beam of $\lambda = 633$ nm and fixed angle at $\theta = 173°$ at 20 °C). The z-average hydrodynamic diameter measured in DLS is derived from the first cumulant of the cumulant fitting of the autocorrelation function. Diffusion coefficient has been transformed to hydrodynamic diameter by using the Stokes-Einstein equation [14]; each result consisting of ten stacked individual measurements of 10 seconds each. We report the hydrodynamic size as hydrodynamic radius, $R_{h,DLS}$ in the manuscript. The ζ-potential of the particles was obtained by Laser Doppler Anemometry and derived from the measured electrophoretic mobility applying

the Smoluchowski approximation. There was no further dilution of the separated particles for DLS measurement, except for internal reference (diluted with MilliQ water at ratio of 1:10).

2.4.3 Electron microscopy examination

The particle´s morphology was investigated by scanning transmission electron microscope (HD-2700Cs, Hitachi, Japan and/or FEI, TALOS F200X) with 200 kV acceleration voltage. Samples for analyses were prepared by direct on-grid centrifugation using carbon-coated copper grids (Quantifoil, DE) [15]. Images were recorded using a high-angle annular dark field (HAADF) detector. The elemental composition of particles was determined using an energy dispersive X-ray detector (EDX) and the spectra were recorded and processed using Digital Micrograph.

2.4.4 AF^4-MALS and AF^4-ICP-MS

Particle fractionation and particle sizing was carried out using an Eclipse Dualtec AF^4 system (Wyatt Technology, Dernbach, Germany) coupled to a MALS detector (DAWN® EOS™, Wyatt Technology Europe GmbH, Dernbach, Germany) and an ICP-MS (Agilent 8800, Agilent, USA). The experimental conditions for the AF^4 experiments and for the ICP-MS measurements are summarized in Table 1.

For the AF^4 experiments, 100 µL of the sample were injected with a large volume injection loop with a maximum injection volume of 900 µL (Agilent G2260A, Agilent, USA). The MALS detector was operated with 17 + 1 observation angles (15 usable in aqueous medium with online DLS attached to angle 11) and a linear polarized laser at 658 nm (DAWN® EOS™, Wyatt Technology Europe GmbH, Dernbach, Germany). The data acquisition interval was set to 2 seconds.

The ICP-MS instrument coupled to the AF^4 was used to quantify the mass concentration of the Ti and Fe eluting from the AF^4 which were then converted to TiO_2 and Fe_2O_3 masses. To reduce the flow entering the ICP-MS nebulizer, the liquid flow from the online MALS detector was split using a peristaltic pump, one branch was directed towards to the ICP-MS (30% or 0.36 mL/min) and the other branch was going to the waste. The flow was continuously monitored by a micro flow meter (TruFlo Sample Monitor 0 - 4.0 mL/min, Glass Expansion, Melbourne, Australia).

The ICP-MS measurements were calibrated using dissolved Ti and Fe standards. A background solution of 0.025% (v/v) FL-70™ was used during Ti and Fe calibration of the ICP-MS to increase solution pH and take into account any possible interferences and matrix effects arising

from the constituents of FL-70^{TM} in the AF^4 carrier. Concentration of the calibration standards included 0; 2.5; 5; 10; 25; 50 and 100 µg/L for Ti and Fe.

3 TiO_2 mass quantification and particle size distribution in sunscreen

3.1 Recovery calculation

NP extraction methods were evaluated based on Ti bulk mass recovery (derived from ICP-MS measurements) and particle specific recovery (derived from light scattering measurements, detector at 90° angle and the ICP-MS signal). Ti bulk mass recovery was calculated from the Ti mass in the extracted suspension and the total Ti mass in the sunscreen. Two particle specific recovery parameters are reported: (i) Rec-MALS: Recovery was determined from the area under peak of the MALS (90°) signal with cross-flow and without crossflow. (ii) Rec-ICP-MS: While this signal is not specific for TiO_2-NPs but sensitive to all particulate material the specific TiO_2-NP recovery was additionally determined by online ICP-MS analysis (Rec-ICP-MS). The Ti and Fe mass eluting from the AF^4 was compared with the total Ti and Fe mass in the sample (Table 1).

3.2 Particle sizing

A purpose of this study was to demonstrate particle size determination with AF^4 based on size calibration and to verify AF^4 sizing by online MALS measurements.

3.2.1 Particle size calibration of AF^4 retention times

Polystyrene latex beads (PS) with certified sizes of 25, 50, 75 and 100 nm radius (hydrodynamic radius) were injected in the AF^4. Retention time of each standard was determined and particle size was calibrated against retention time. The mass of the injected PS particles was set to 0.5, 0.25, 0.1 and 0.1 µg to correspond to the size-selective sensitivity of the MALS detector (90°). Limits of quantification for particle concentration and particle size are summarized in SI.3.

Based on this size calibration the PSD was either expressed as intensity-based PSD based on the MALS 90° signal or mass-based PSD based on the ICP-MS signal. For the conversion of element masses recorded by the ICP-MS instrument to particle masses, a constant stoichiometry (TiO_2 and Fe_2O_3) was assumed and retention times were corrected for the delay between MALS and ICP-MS detector.

3.2.2 Evaluation of the MALS signal for orthogonal particle sizing

The hydrodynamic particle size was verified by the MALS signal of 15 detector angles. These data were used to calculate the radius of gyration (R_{rms}) of the particles by fitting the recorded light scattering intensities to a particle scattering function. To select the most appropriate scattering function we evaluated different data processing algorithms including Berry (linear), Debye (3rd order), Zimm (linear) and Random coil. This sizing approach is referred to internal orthogonal particle sizing. The ratio of R_{rms} over R_h also known as shape factor provides information on particle shape. The value of the shape factor indicates to what extent particles deviate from a sphere. The R_{rms}/R_h ratio of a sphere is 0.775 [16,17] and Gogos et al. [18]describe how it changes when moving to a rod-like particle.

4 Results and Discussion

4.1 Selection of the MALS data processing algorithm for internal orthogonal particle sizing

The most suitable algorithm for processing the entire MALS data was selected based on the evaluation of R_{rms} values obtained from pristine TiO_2-NPs suspension. R_{rms} values and respective R_{rms}/R_h ratios were calculated with the processing algorithms and plotted against the R_h value obtained from AF^4 calibration (Fig.S2a, b). All algorithms (Berry (linear), Debye (3rd order), Zimm (linear) and Random coil) returned very comparable R_{rms} values for small particles (R_{rms} < 30 nm) (Fig. S2a). For larger particles up to 100 nm, the R_{rms} values were similar between algorithms, except for Debye, which calculated smaller particle sizes. For the particle size range between 30 and 100 nm R_{rms} values increased linearly with increasing R_h indicating ideal particle elution in the AF^4 [14,17]. For particles R_h > 100 nm Zimm, Debye and Berry algorithm resulted in considerable deviations from the R_h data (e.g. R_h=110 nm, Zimm fit R_{rms}≈250 nm), due to poor fittings of the strong curvature of R(θ) for the larger particles, especially when they are homogeneous spheres. However, these algorithms calculate the R_{rms} regardless of the geometry of the particles. Among those Zimm fit gives the best approximations for R(θ) with particle sizes up to 100 nm in diameter. [17]. The random coil algorithm is a nonlinear function used for particles with known geometries similar to proteins [14]. Therefore, it was not used in this study, but the Zimm algorithm was selected. For the particle size range below 100 nm the Zimm fit may

be applicable to verify R_h data determined by AF^4 calibration although it is inappropriate to characterize larger particles (> 100 nm).

4.2 PSD of the pristine TiO_2-NP suspension

The conditions for the AF^4 experiments were optimized with respect to void peak separation, retention time, particle recovery and calibrated size range (R_h = 25-100 nm) (Table 2). This parameter set was previously suggested by Loeschner et al. [19] to evaluate AF^4 particle size separation conditions [19]. Under optimized conditions the TiO_2 particle recovery was above 90% (Table 3) and retention was maximized.

The mass-based PSD of pristine TiO_2-NP suspension was mono-modal ($R_{h,mode(ICP-MS)}$=40 nm). It spanned from 10 nm to 150 nm and exhibited a slight tailing (d_{10} = 27 nm; d_{90} = 87nm). Therefore, $R_{h,mode(ICP-MS)}$ and $R_{h,median(ICP-MS)}$ differed slightly (Table 3). The intensity-based PSD obtained from MALS was also mono-modal and its mode was shifted towards a larger R_h ($R_{h,mode(MALS)}$=57 nm) compared to the mode of the mass-based PSD (Fig. 1a). This difference is explained by a disproportionate increase in the intensity of the MALS signal with increasing particle size [14]. Thus, the intensity-based PSD is always shifted towards larger particle size compared to the mass-based PSD. The median particle size of the intensity-based PSD (Table 3) is consistent with the intensity-based DLS results from batch measurements of the TiO_2 suspension (Table S1).

The R_{rms} data increased linearly with increasing R_h until R_h in approximately 80 nm (Fig. 1a); accordingly, the R_{rms}/R_h ratio remained constant in the size range and a constant R_{rms}/R_h ratio during elution of uniformly shaped particles can indicate ideal separation conditions. Based on the R_{rms}/R_h ratios > 0.775 obtained for the sample (Fig. S3a) it is assumed that TiO_2-NPs are non-spherical. The shape factor of spherical particles equals 0.775 and non-spherical particles as rods and plates exhibit shape factors > 0.775 [20]. For larger particle sizes R_{rms} continued to increase disproportionally with R_h (Fig. 1a); the shape factor also increased accordingly before decreasing again (Fig. S3a). With regard to electron microscopy images obtained from literature we expect TiO_2 particles present as aggregates [21]; hence R_{rms}/R_h ratios > 0.775 are expected. For larger particles, however, the strong deviation of R_{rms} from R_h and the associated development of R_{rms}/R_h ratios is due to the inability of Zimm algorithm to correctly describe particles > 100 nm.

4.3 Performance of the sample preparation methods

All three sample preparation methods 1, 2 and 3 were assessed regarding their applicability for extraction of pristine TiO_2-NP from the sunscreen formulation. In the following section we present TiO_2-NP recovery data followed by the mass- and intensity-based TiO_2 PSDs.

4.3.1 Mass recovery of the spiked sunscreen formulation

Ti bulk mass recoveries exceeded 70% for all three methods. Highest Ti bulk mass recovery was achieved using method 2 (combustion) followed by method 1 (ultracentrifugation + hexane washing) and method 3 (dilution followed by particle stabilization) (Table 3). Particle specific recoveries after size separation were between 71% and 91% for all methods (Table 3). Surprisingly, the unspecific Rec-MALS was always lower than the Ti specific Rec-ICP-MS, indicating losses of the non-Ti particulate matrix components in the AF^4 system that remain after sample preparation. The obtained particle recovery exceeded previously reported values of approximately 50%, e.g. supercritical fluid extraction [9]. High recoveries in FFF separations is important, since losses are often not equally distributed across the size distribution and a specific fraction of the sample might be lost (in most cases the larger particles suffer higher losses) that would lead to a misrepresentation of the original PSD.

4.3.2 Particle size distribution of the spiked sunscreen formulation

When interpreting the sizing data, it must be acknowledged that light scattering based methods such as DLS and MALS are not specific for the target particles (TiO_2) but are reporting the size distribution of the target particles and any other particulate component, might it be remainders from the emulsion matrix, micelles of the surfactants or other particles in the sample as stabilizers or pigments.

The stability of pristine TiO_2-NP suspension and suspensions resulting from method 1, 2 and 3 was initially verified over 60 minutes by batch DLS analysis (Table S1). Method 2 provided the least stable suspension as the particle size increased by more than 8% and polydispersity index increased from 0.21 to 0.28 within the test period. The combustion process removed the organic matrix components and thus the stabilizing effects of organic residues.

The mode and the width of the mass-based PSD of the suspension obtained with method 1 and method 2 increased compared to the PSD of the pristine TiO_2-NPs suspension. For instance, the $R_{h,mode}$ of extracted TiO_2-NP was 72 nm (method 1) whereas the mode of the pristine TiO_2 NP

suspension was 40 nm (Table 3). The width of the PSD expressed as difference between d_{90} and d_{10} increased as well (Table 3, Fig. 1). Injection of large aggregates into the AF^4 system likely led to a loss of the particles by deposition on the AF^4 membrane [19,22,23]resulting in decreased TiO_2 recoveries and alteration of the PSD [8] which was also observed in our data set.

However, a different observation was made for method 3. No increase in particle size was found; contrary, a slight decrease of the mode of the mass-based PSD to $R_{h,mode}$ = 30 nm was determined. Its width remained unchanged as the shape slightly changed and a tailing occurred. Comparing the mass- and intensity-based PSD the first peak is devoted to TiO_2-NPs while the second peak of the intensity-based PSD may be partially attributed to remaining organic sunscreen constituents after dilution. This is supported by sunscreen blank analysis where the MALS signal (90°) indicates the presence of particulate constituents whereas the Ti-signal does not reflect the presence of TiO_2 particles (Fig. S5). Hence, both TiO_2-NPs and other, non-Ti particulate constituents are present in the suspension resulting from method 3.

Our results show that sample preparation method 3 did not significantly alter the size of spiked TiO_2-NPs compared to the pristine TiO_2-NPs formulation, whereas method 1 and 2 resulted in broadening of the PSD of TiO_2 and an increase in TiO_2 particle size. These alterations may be a result of sample preparation and the inability of method 1 and 2 to sufficiently stabilize TiO_2-NPs. Further, the particle suspension resulting from method 2 was least stable compared to method 1 and 3. A particle size increase has been reported previously and was explained by alteration of particle size due to aggregation during sample preparation [7,9,24].

4.3.3 Evaluation of the MALS signal for orthogonal particle sizing

For suspensions prepared with method 1 and method 3, we observed an inversion of the R_{rms} evolution in the region R_h < 30 nm (Fig. 1 b, d). This non-ideal behavior can be explained by the elution of larger particles which were not retained in the AF^4 channel and therefore, may overlap with the main peak region. The linear increase in R_{rms} over R_h spans from approximately 30 nm to ≈ 80 nm for suspensions resulting from method 1 and 2 and to approximately 70 nm for suspension resulting from method 3 (Fig. 1). This indicates that the size fractionation was controlled by particle diffusion in this size range of the PSD. The linear increase of R_{rms} for method 3 covered the entire mass-based PSD for TiO_2-NPs. The PSDs in suspensions prepared with method 1 and 2 are broader and we observed a non-linear increase of the R_{rms} data for

particle sizes > 80 nm (Fig. 1 b, c). This can be attributed to the inability of the linear Zimm algorithm to fit larger particle sizes of TiO_2-NPs agglomerates [17] and to the existence of larger particulate matrix components other than TiO_2-NP which have a different elution behavior (possibly undergoing steric elution) in the AF^4 channel. Only suspensions extracted with method 1 revealed a constant R_{rms}/R_h ratio for R_h < 80 nm (Fig. 4). For suspensions obtained with method 2 and 3 we found a moderate increase in R_{rms}/R_h ratio from 0.9 to 1.5. This may be either due to a change in particle shape and particle aspect ratio or an overestimation of R_{rms} for particle sizes above 80 nm (Fig. S4), especially in method 3 where the presence of non-Ti particulate matrix components might interfere with the MALS analysis and the selected data treatment (linear Zimm). We believe that the latter is the reason for the higher values of R_{rms}/R_h. It may be concluded that the inability of calculating R_{rms} radii > 80 nm by the available fitting algorithms is an inherent challenge when using MALS data for orthogonal sizing.

4.4 Application of method 1 and 3 to sunscreen samples

Method 1 and 3 were applied to sunscreen A and B, the two samples resembling typical market products. Although TiO_2-NP recoveries of method 2 were comparable with methods 1 and 3, particle stability was lower (Table S1). Therefore, method 2 was not applied to sunscreen samples. We determined the Ti-mass and particle recovery, the PSDs of the extracted suspensions and applied the orthogonal sizing approach to approve ideal separation conditions in the AF^4.

4.4.1 Mass recovery

Ti bulk mass recovery for sunscreen A and sunscreen B was > 73% (Table 3). This shows that preparation methods 1 and 3 were able to extract TiO_2 from the sunscreen matrix. Comparable results were obtained for the particle recovery based on light scattering intensity and mass (Table 3).

4.4.2 Particle size distribution of sunscreen samples

Particle size screening with DLS-batch measurements of sunscreen A and B showed smaller average particle sizes in suspensions obtained with method 1 ($R_{h,DLS}$=109 nm) compared to method 3 ($R_{h,DLS}$=182 nm) (Table S1). Insufficient particle stability after sample preparation,

however, has been excluded in both cases as the particle size did not increase within 60 min of DLS-batch analysis.

Sunscreen A – simple sunscreen – only UV-filter TiO_2 in a sunscreen formulation as matrix

Mass-based PSDs of sunscreen A was mono-modal for both methods (Fig. 2). The mode values of the mass-based TiO_2 PSD, inferred from the Ti signal were 42 nm, and 38 nm with method 1 and 3, respectively. Intensity-based PSDs of sunscreen were slightly shifted to larger particle sizes compared to the mass-based PSDs in both cases (Table 3). A mono-modal intensity-based PSD was observed for suspensions resulting from methods 1 for sunscreen A. However, the PSD of the suspension resulting from sunscreen A following method 3 revealed a second peak at around 150 nm (Fig. 2c). This second peak was not observed in the Ti mass-based PSD. Therefore, particulate organic residuals may have been present in sunscreen A too; similar to the observations made from the spiked sunscreen sample (Fig. 1d).

Sunscreen B – similar to commercial product

The TiO_2 mass-based PSD obtained from sunscreen B with method 1 exhibited a tailing (Fig. 2 b, light grey histogram). For the suspension extracted with method 3 a bimodal TiO_2 mass-based PSD was obtained indicating a second population of TiO_2-NP sizes (Fig. 2 d, light grey histogram). In parallel the Fe signal was monitored and it revealed an iron-containing particle population with R_h values larger than 100 nm for suspensions extracted with method 1 and 3 (Fig. 2 b, d, the light grey histogram). The non-specific intensity based PSDs of suspensions extracted from sunscreen B with method 1 and 3 were bimodal too, confirming the results obtained from the mass-based PSD (AF^4-ICP-MS) (Fig. 2 b, d). Particles containing Ti and Fe were assigned to the second peak of the intensity-based PSD (Fig. 2 b, d, the light grey and grey histogram), which can be explained either by associations between Fe_2O_3-NPs and TiO_2-NPs or by the presence of individual TiO_2 and Fe_2O_3-NPs. However, the AF^4-ICP-MS experimental setup did not allow differentiating between both.

The sizing of the second peak is challenging for several reasons. First, there is no MALS signal available because particles are already larger than working range of the MALS system (particles are >100 nm). Second, EM data of the extracted suspensions from sunscreen B suggest that iron oxide and TiO_2 particles extend into a size above the calibrated size range of the AF^4 channel (Fig. 3). In sunscreen B elongated TiO_2-NPs with size of approximately 50 nm and larger

irregular shaped TiO_2 particle aggregates/agglomerates with sizes between 200 and 300 nm were identified during EM-EDX investigations (Fig. 3). Iron oxide particles with sizes > 1 µm were also observed by EM. It is conceivable that the tailing of the TiO_2 PSD > 100 nm observed in sample sunscreen B originates from this second type of TiO_2 particles (pigment-grade TiO_2) present in the sample. Commonly sizes of TiO_2 pigment particle are well above 100 nm whereas UV filter capabilities are most efficient in the range of 30 to 50 nm [25]. Elution behavior of Fe oxide particles does not correspond to the particle size observed by EM. For spherical particles with sizes > 800 nm elution is controlled by steric effects and no longer by diffusion (Fig. S1). In such cases where large and small particles are present in the same sample Brownian (diffusion) mode and steric elution mode occurs in parallel making correct particle sizing by AF^4 impossible. However, MALS data prove that the small TiO_2 fraction < 100nm (radius) is still sized correctly (details in 4.4.3). In the present study, rod-like Fe-oxide particles > 1000 nm (Fig. 2) suggest that a correct particle sizing of Fe-oxides based on AF^4-MALS and AF^4-ICP-MS is not possible, although they appear in the fractogram.

4.4.3 Evaluation of the MALS signal of sunscreen samples for orthogonal particle sizing

The R_{rms} data of the particle suspensions extracted from sunscreen A applying method 1 and 3 showed a linear increase with increasing R_h in a size range between 25 nm and 80 nm (Fig. 2 a, c) representing the size region of the main peak. The linear increase in R_{rms} indicates ideal elution of particles in this size range. For R_h > 80 nm the R_{rms} increase was disproportionate. Similar as for the suspensions extracted from sunscreen A we found for sunscreen B that the R_{rms} increased linearly up to $R_h \approx 80$ nm followed by a disproportionate increase. However, the conclusion that particle > 80 nm do not follow ideal separation is not possible because the Zimm extrapolation algorithm is not suitable for particles in this size range.

The R_{rms}/R_h ratio slightly increased in the R_h range from 25 to 80 nm for suspension extracted from sunscreen A and sunscreen B (Fig. S4). For R_h > 75/80 nm values the R_{rms}/R_h ratios deviate from the expected behaviour for both sunscreens for several reasons. First a steeper increase above 100 nm R_h would be expected, since from this particle size on the separation mode of this FFF method transits from Brownian to steric mode (Figure S1) and while the R_h stems from a linear calibration not considering this and R_{rms} is a measure of the actual (larger) particle size, R_{rms}/R_h increases with higher slope than in the purely Brownian mode separation range (Figure

S4 c, d). Second, particle morphology or/and size might increase above the limit where a linear Zimm fit can still produce accurate R_{rms} (Figure S4 a, b). Third low scattering intensities lead to higher noise, especially in the smaller angles which are most important for the determination of R_{rms}, which leads to wrong R_{rms} or high variations in R_{rms} (Fig. S4 a, c).

Conclusively, particles size validation for real samples can be performed for particles with R_h < 80 nm. The major limitation of this approach is the applicability of the MALS data for a restricted calibrated particle size range in the AF^4.

4.5 Implications of the regulatory framework for the analytical methodology

Current cosmetic products regulation defines nanomaterials as insoluble or biopersistent and intentionally manufactured material with at least one external dimension between 1 and 100 nm (Products Regulation 1223/2009) [1] which implies that every ingredient that has particles in this size range (and is biopersistent and insoluble) would qualify as nanomaterial with the respective labeling obligations. Cosmetic product regulation demands a premarket notification for nanomaterial containing cosmetic products [1]. The notification includes the identification of the nanomaterial and its specifications including particle size, physical and chemical properties, estimation of the quantity of nanomaterial in the product, as well as toxicological, safety and exposure data [26]. Ultimately, this definition relies on the capabilities of analytical methods to measure to what extent nanoparticles are present in a product and thus to assess whether a material is classified as a nanomaterial.

The methodology and workflow for the measurement of nanoparticles in suspensions as presented here can be applied to determine the PSD of pristine particle suspensions and particles incorporated in a cosmetic product matrix. The latter is required to enforce product labelling according to cosmetic product regulation. In the presented case study the $R_{h,median}$ of sunscreen A is 42 nm (or 84 nm in diameter) and of sunscreen B $R_{h,median}$ is 50 nm (or 100 nm in diameter). According to these results both sunscreens contain nanoparticles and would thus be classified as nanomaterials. Even under the current EC recommendation for a definition of nanomaterials, where decision is based on > 50% of the number-based distribution (median of the number-based distribution < 100 nm), the analyzed ingredient TiO_2 would qualify as a nanomaterial, since conversion from mass-based to number-based distribution would further decrease the median value.

In case the tailing (Fig. 2b) is due to a different particle type of the same chemical identity (a different nanoform) a differentiation between both particle types would be required for a correct classification. Such a differentiation is not possible using solely elemental detection with ICP-MS.

5 Conclusion

Data as presented in this study are urgently required by current cosmetic product regulation demanding both characterization of pristine nanomaterials and nanomaterials in cosmetic products. Three sample preparation methods (ultracentrifugation and hexane washing, thermal destruction of the matrix and surfactant assisted particle extraction followed by dilution) were evaluated regarding their suitability to extract and quantify TiO_2-NPs in sunscreens. The latter (method 3) was most efficient in terms of TiO_2 particle recovery and affected the PSD the least. The method can be considered as simple, since it is based on dilution. With this sample preparation method, particle recoveries were achieved in the range of 70 to 100% which is significantly higher compared to previously reported recoveries. Using control samples with known TiO_2-NP concentrations confirmed that particle size alterations following matrix dilution with subsequent particle stabilization were negligible.

The MALS signal proved to be applicable as an orthogonal particle sizing method allowing the verification of good particle separation in the AF^4, the range of certainty and disclosed interferences/artefacts as well as the boundaries of the application.

Finally, a comprehensive intra-laboratory assessment of the method was performed to determine data uncertainties and will be submitted as a separate manuscript.

Acknowledgment

This research has received funding from the European Union's Seventh Program for research, technological development and demonstration under grant agreement No 604347-2. The authors acknowledge support of the Scientific Center for Optical and Electron Microscopy ScopeM of the Swiss Federal Institute of Technology ETHZ.

References

[1] EC, Cosmetic Products Regulation 1223/2009, THE EUROPEAN PARLIAMENT AND

OF THE COUNCIL, 2009.

[2] H. Stamm, N. Gibson, E. Anklam, Detection of nanomaterials in food and consumer products: Bridging the gap from legislation to enforcement, Food Addit. Contam. - Part A Chem. Anal. Control. Expo. Risk Assess. 29 (2012) 1175–1182. https://doi.org/10.1080/19440049.2012.689778.

[3] S. Wagner, S. Legros, K. Loeschner, J. Liu, J. Navratilova, R. Grombe, T.P.J. Linsinger, E.H. Larsen, F. von der Kammer, T. Hofmann, First steps towards a generic sample preparation scheme for inorganic engineered nanoparticles in a complex matrix for detection, characterization, and quantification by asymmetric flow-field flow fractionation coupled to multi-angle light scattering and , J. Anal. At. Spectrom. 30 (2015) 1286–1296. https://doi.org/10.1039/C4JA00471J.

[4] K. Loeschner, J. Navratilova, R. Grombe, T.P.J. Linsinger, C. Købler, K. Mølhave, E.H. Larsen, In-house validation of a method for determination of silver nanoparticles in chicken meat based on asymmetric flow field-flow fractionation and inductively coupled plasma mass spectrometric detection, Food Chem. 181 (2015) 78–84. https://doi.org/10.1016/j.foodchem.2015.02.033.

[5] M. Mattarozzi, M. Suman, C. Cascio, D. Calestani, S. Weigel, A. Undas, R. Peters, Analytical approaches for the characterization and quantification of nanoparticles in food and beverages, Anal. Bioanal. Chem. 409 (2017) 63–80. https://doi.org/10.1007/s00216-016-9946-5.

[6] C. Contado, A. Pagnoni, TiO2 in commercial sunscreen lotion: Flow field-flow fractionation and ICP-AES together for size analysis, Anal. Chem. 80 (2008) 7594–7608. https://doi.org/10.1021/ac8012626.

[7] V. Nischwitz, H. Goenaga-Infante, Improved sample preparation and quality control for the characterisation of titanium dioxide nanoparticles in sunscreens using flow field flow fractionation on-line with inductively coupled plasma mass spectrometry, J. Anal. At. Spectrom. 27 (2012) 1084. https://doi.org/10.1039/c2ja10387g.

[8] I. López-Heras, Y. Madrid, C. Cámara, Prospects and difficulties in TiO2 nanoparticles analysis in cosmetic and food products using asymmetrical flow field-flow fractionation hyphenated to inductively coupled plasma mass spectrometry, Talanta. 124 (2014) 71–78. https://doi.org/10.1016/j.talanta.2014.02.029.

[9] D. Müller, S. Cattaneo, F. Meier, R. Welz, T. de Vries, M. Portugal-Cohen, D.C. Antonio, C. Cascio, L. Calzolai, D. Gilliland, A. de Mello, Inverse supercritical fluid extraction as a sample preparation method for the analysis of the nanoparticle content in sunscreen agents, J. Chromatogr. A. 1440 (2016) 31–36. https://doi.org/10.1016/j.chroma.2016.02.060.

[10] A. Philippe, J. Košík, A. Welle, J.-M. Guigner, O. Clemens, G.E. Schaumann, Extraction and characterization methods for titanium dioxide nanoparticles from commercialized sunscreens, Environ. Sci. Nano. (2018). https://doi.org/10.1039/C7EN00677B.

[11] A. Samontha, J. Shiowatana, A. Siripinyanond, Particle size characterization of titanium dioxide in sunscreen products using sedimentation field-flow fractionation-inductively coupled plasma-mass spectrometry, Anal. Bioanal. Chem. 399 (2011) 973–978. https://doi.org/10.1007/s00216-010-4298-z.

[12] C. Cascio, O. Geiss, F. Franchini, I. Ojea-Jimenez, F. Rossi, D. Gilliland, L. Calzolai, Detection, quantification and derivation of number size distribution of silver nanoparticles in antimicrobial consumer products, J. Anal. At. Spectrom. 30 (2015) 1255–1265. https://doi.org/10.1039/C4JA00410H.

[13] C. Contado, L. Ravani, M. Passarella, Size characterization by Sedimentation Field Flow Fractionation of silica particles used as food additives, Anal. Chim. Acta. 788 (2013) 183–192. https://doi.org/10.1016/j.aca.2013.05.056.

[14] S. Podzimek, Light Scattering, Size Exclusion Chromatography and Asymmetric Flow Field Flow Fractionation: Powerful Tools for the Characterization of Polymers, Proteins and Nanoparticles, 2011. https://doi.org/10.1002/9780470877975.

[15] D. Mavrocordatos, C.P. Lienemann, D. Perret, Energy-filtered transmission electron-microscopy for the physicochemical characterization of aquatic submicron colloids, Mikrochim. Acta. 117 (1994) 39–47.

[16] M. Baalousha, F. V.D. Kammer, M. Motelica-Heino, H.S. Hilal, P. Le Coustumer, Size fractionation and characterization of natural colloids by flow-field flow fractionation coupled to multi-angle laser light scattering, J. Chromatogr. A. 1104 (2006) 272–281. https://doi.org/10.1016/j.chroma.2005.11.095.

[17] F.V.D. Kammer, M. Baborowski, K. Friese, Field-flow fractionation coupled to multi-angle laser light scattering detectors: Applicability and analytical benefits for the analysis

of environmental colloids, Anal. Chim. Acta. 552 (2005) 166–174. https://doi.org/10.1016/j.aca.2005.07.049.

[18] K. Loeschner, J. Navratilova, S. Legros, S. Wagner, R. Grombe, J. Snell, F. von der Kammer, E.H. Larsen, Optimization and evaluation of asymmetric flow field-flow fractionation of silver nanoparticles, J. Chromatogr. A. 1272 (2013) 116–125. https://doi.org/10.1016/j.chroma.2012.11.053.

[19] K. Loeschner, J. Navratilova, C. Købler, K. Mølhave, S. Wagner, F. Von Der Kammer, E.H. Larsen, Detection and characterization of silver nanoparticles in chicken meat by asymmetric flow field flow fractionation with detection by conventional or single particle ICP-MS, Anal. Bioanal. Chem. 405 (2013). https://doi.org/10.1007/s00216-013-7228-z.

[20] A. Gogos, R. Kaegi, R. Zenobi, T.D. Bucheli, Capabilities of asymmetric flow field-flow fractionation coupled to multi-angle light scattering to detect carbon nanotubes in soot and soil, Environ. Sci. Nano. 1 (2014) 584–594. https://doi.org/10.1039/C4EN00070F.

[21] K. Rasmussen, J. Mast, P.-J. De Temmerman, E. Verleysen, N. Waegeneers, F. Van Steen, J.C. Pizzolon, L. De Temmerman, E. Van Doren, K.A. Jensen, R. Birkedal, M. Levin, S.H. Nielsen, I.K. Koponen, P.A. Clausen, V. Kofoed-Sørensen, Y. Kembouche, N. Thieriet, O. Spalla, C. Guiot, D. Rousset, O. Witschger, S. Bau, B. Bianchi, C. Motzkus, B. Shivachev, L. Dimowa, R. Nikolova, D. Nihtianova, M. Tarassov, O. Petrov, S. Bakardjieva, D. Gilliland, F. Pianella, G. Ceccone, V. Spampinato, G. Cotogno, N. Gibson, C. Gaillard, A. Mech, Titanium Dioxide, NM-100, NM-101, NM-102, NM-103, NM-104, NM-105: Characterisation and Physico- Chemical Properties, 2014. https://doi.org/10.2788/79554.

[22] F. von der Kammer, S. Legros, T. Hofmann, E.H. Larsen, K. Loeschner, Separation and characterization of nanoparticles in complex food and environmental samples by field-flow fractionation, TrAC - Trends Anal. Chem. 30 (2011) 425–436. https://doi.org/10.1016/j.trac.2010.11.012.

[23] B. Schmidt, J.H. Petersen, C. Bender Koch, D. Plackett, N.R. Johansen, V. Katiyar, E.H. Larsen, Combining asymmetrical flow field-flow fractionation with light-scattering and inductively coupled plasma mass spectrometric detection for characterization of nanoclay used in biopolymer nanocomposites, Food Addit. Contam. - Part A Chem. Anal. Control. Expo. Risk Assess. 26 (2009) 1619–1627. https://doi.org/10.1080/02652030903225740.

[24] Y. Dan, H. Shi, C. Stephan, X. Liang, Rapid analysis of titanium dioxide nanoparticles in sunscreens using single particle inductively coupled plasma-mass spectrometry, Microchem. J. 122 (2015) 119–126. https://doi.org/10.1016/j.microc.2015.04.018.

[25] P.M. Hext, J.A. Tomenson, P. Thompson, Titanium dioxide: Inhalation toxicology and epidemiology, Ann. Occup. Hyg. 49 (2005) 461–472. https://doi.org/10.1093/annhyg/mei012.

[26] H. Rauscher, K. Rasmussen, B. Sokull-Klüttgen, Regulatory Aspects of Nanomaterials in the EU, Chemie-Ingenieur-Technik. 89 (2017) 224–231. https://doi.org/10.1002/cite.201600076.

Table 1. List of samples used in this study.

Table 2. Experimental parameters for AF4 experiments and ICP-MS measurements used for TiO_2 and Fe_2O_3 NPs characterization.

Fig. 1. PSD as hydrodynamic radius based on ICP-MS and light scattering signal as well as R_{rms} of pristine TiO_2-NP with a concentration of 1 %w/v dispersed in 1% v/v SDS (a), spiked sunscreen formulation sample using method 1 (b), method 2 (c), and method 3 (d).

Table 3. Measured and calculated results based on the three criteria. The data are calculated from MALS and ICP-MS fractograms.

Fig. 2. AF4-MALS-ICP-MS fractograms and Rrms of a) TiO_2 particles separated from sunscreen A and b) TiO_2 and Fe_2O_3 particles separated from sunscreen B using method 1.

Fig. 3. Electron microscopy and EDX detection with extracted particles from sunscreen A and B with method 1 and 3. The images of sample B (Fe) were recorded with HD using secondary electron mode (SE).

Sample type		**c(TiO_2) [g L^{-1}]**	**c(Fe_2O_3) [g L^{-1}]**	**Description**
Pristine suspension	TiO_2-NPs	10	-	A suspension of well characterized TiO_2-material (NM-104).
Blank formulation	sunscreen	-	-	Blank, particle-free sunscreen formulation containing no.
Spiked formulation	sunscreen	10	-	Blank sunscreen formulation containing TiO_2-material (NM-104).
Sunscreen A		36	-	Market sunscreen formulation containing nano-size TiO_2 particles.
Sunscreen B		54	13	Market sunscreen formulation containing micro- and nano-size TiO_2 and micro-size Fe_2O_3 particles.

AF^4	**unit**	**value**
Tip to tip chancel length	[cm]	27.5
Spacer	[µm]	350
Focus flow rate	[ml/min]	0.60
Injection flow	[ml/min]	0.1
Injection time	[min]	10
Focus time	[min]	2
Elution time	[min]	40
Detector flow rate	[mL/min]	1
Cross flow rate	[mL/min]	0.6
Membrane		Regenerated cellulose (RC), 10 kDa, Millipore
Carrier		0.025% (v/v) FL-70^{TM}
Injection volume	[µL]	50 of sample suspension
ICP-MS		
RF power	[W]	1600
Sample depth	[mm]	10
Gas flow rates		
-Carrier	[L/min]	1.06
-Dilution	[L/min]	0.35
-Collision gas He	[mL/min]	4.5
Sample uptake rate	[mL/min]	0.3 (established by split flow)
Nebulizer		MICROMIST (Glass Expansion)
Spray chamber		Scott double-pass
Isotopes monitored		^{48}Ti and ^{56}Fe
Dwell time	[ms]	100

Size calibrations of the AF^4 channel were performed under similar run conditions.

Sample	Method	Bulk mass recovery		AF^4-MALS and –ICP-MS recovery			Particle size from AF^4-MALS & ICP-MS			
		Rec-Bulk Ti [%]	Rec-Bulk Fe [%]	Rec-MALS [%]	Rec-ICP-MS Ti [%]	Rec-ICP-MS Fe [%]	$R_{h,\ mode}$ [nm] (MALS)	$R_{h,\ median}$ [nm] (MALS)	$R_{h,\ mode}$ [nm] (ICP-MS)	$R_{h,\ 10}$; $R_{h,median}$; $R_{h,90}$ [nm], (ICP-MS)
Untreated pristine TiO_2		-	-	73	93	-	57	62	40	27/46/87
Spiked sunscreen formulation	1	87	-	71	83	-	91	100	72	34/82/171
	2	104	-	79	91	-	89	95	50	29/68/141
	3	72		79	91		40 and 89	70	30	21/36/98
Sunscreen A	1	77	-	80	83	-	60	66	42	26/48/121
	3	89		80	83		44	45	38	23/42/95
Sunscreen B	1	88	112	70	85	84	65 and 151	111	44	30/54/146
	3	95	86	101	100	84	56 and 126	50	47#	20/50/88#

1: the combination of ultracentrifuge and hexane washing method,

2: thermal combustion method,

3: dilution and stabilization.

 # parameters of first particle size population

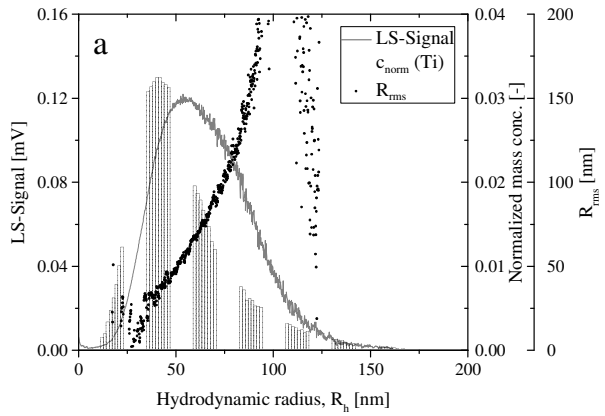

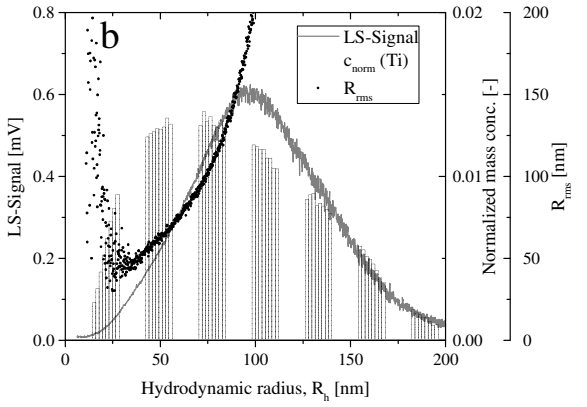

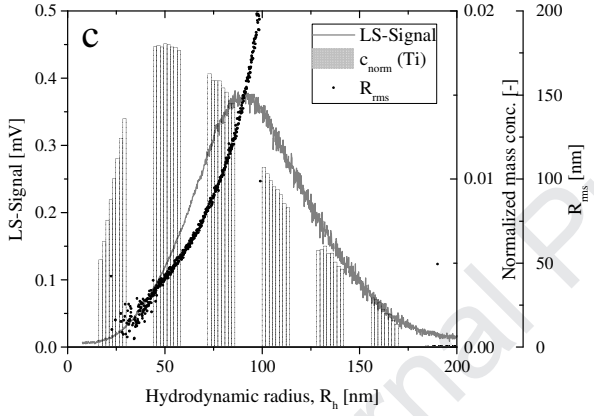

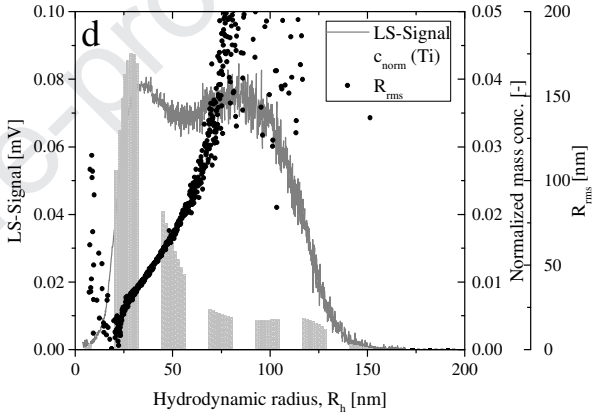

sunscreen A ***sunscreen B***

Method 1

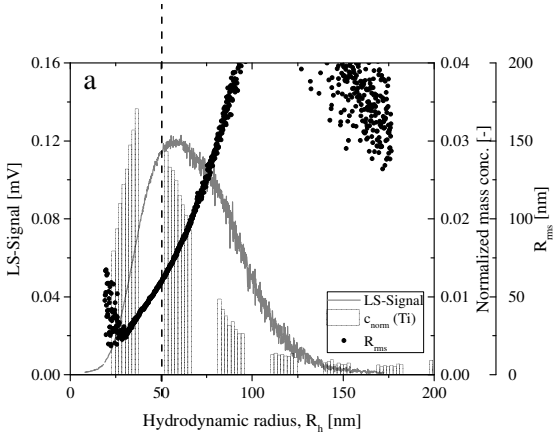

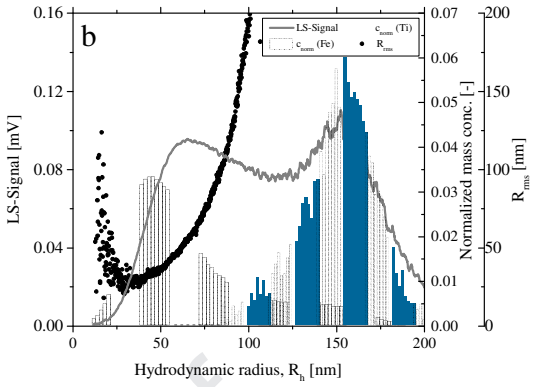

Method 3

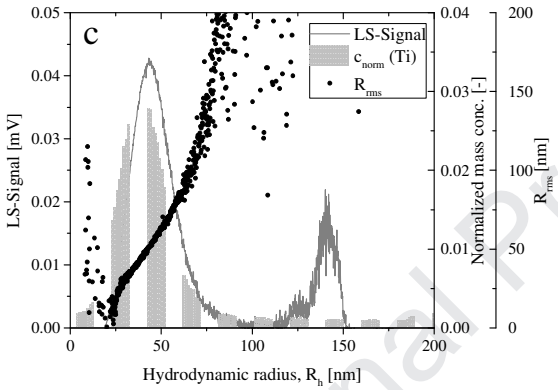

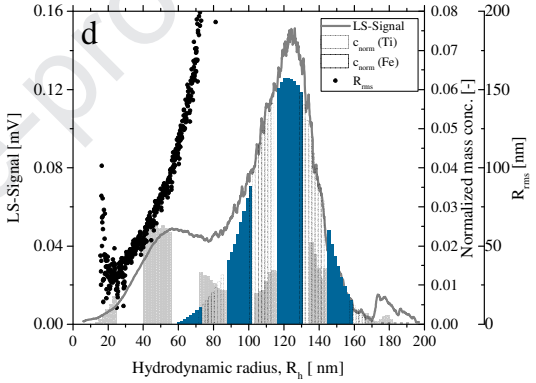

	sunscreen A	***sunscreen B***
Method 1	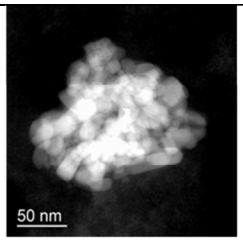 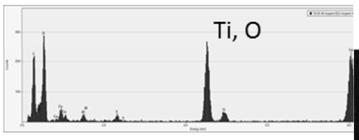	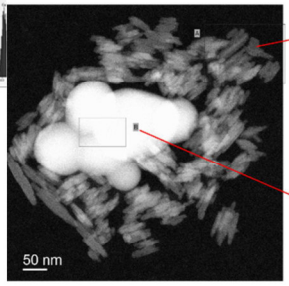 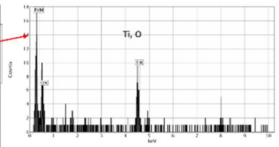 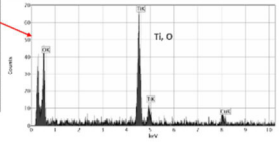 HAADF 180 kX 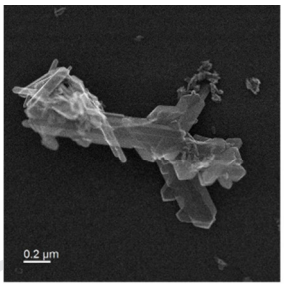 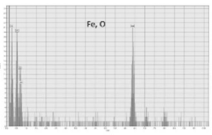 HAADF 50 kX
Method 3	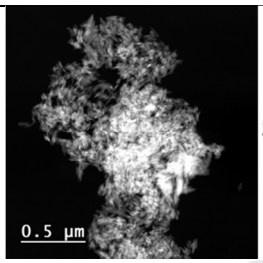 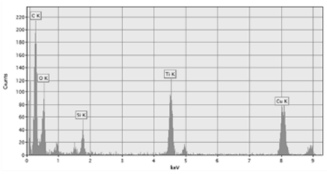	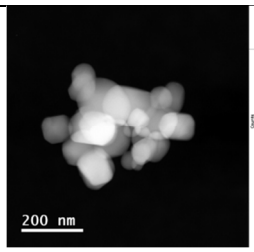 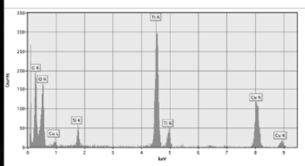 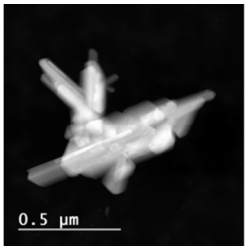 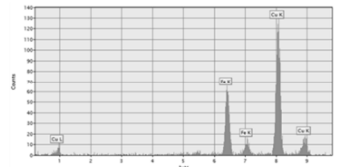

Highlights

- A sample preparation method to assess TiO_2-NPs in sunscreens was identified.
- TiO_2-NPs size was determined with AF4 hyphenated with MALS.
- TiO_2-NPs concentration was determined with AF4 hyphenated with ICP-MS.
- Fitting MALS signal was appropriate orthogonal particle sizing method for NPs.

Author Contributions: conceptualization, Frank von der Kammer, Milica Velimirovic and Stephan Wagner; methodology, Frank von der Kammer; validation Toni Uusimäki, Ralf Kaegi, Milica Velimirovic, Stephan Wagner; formal analysis, Milica Velimirovic, Stephan Wagner, Fazel Abdolahpur Monikh; investigation Milica Velimirovic, Stephan Wagner, Fazel Abdolahpur Monikh, Toni Uusimäki; resources, Frank von der Kammer, Thilo Hofmann; writing-original draft preparation, Milica Velimirovic, Stephan Wagner; writing-review and editing, Frank von der Kammer, Thilo Hofmann, Ralf Kaegi; project administration, Milica Velimirovic, Stephan Wagner; funding acquisition, Frank von der Kammer, Thilo Hofmann

Declaration of interests

☒ The authors declare that they have no known competing financial interests or personal relationships that could have appeared to influence the work reported in this paper.

☐The authors declare the following financial interests/personal relationships which may be considered as potential competing interests: